**Proceedings of the ASME 2019
International Mechanical Engineering Congress and Exposition
IMECE2019
November 11-14, 2019, Salt Lake City, UT, USA**

IMECE2019-11015

STUDY OF TWO-DIMENSIONAL FLOW-BOILING MORPHOLOGICAL CHARACTERISTICS IN THE MICRO GAP WITH SURFACE WETTABILITY ON HOT SPOT

Anwarul Karim[1] and Jong-Hoon Kim[1].
[1]Department of Mechanical Engineering, Washington State University, Vancouver, WA, 98686, United States

ABSTRACT

Thermal management is one of the most challenging problems of electronic devices today. As technology becomes increasingly miniaturized, extremely localized heat dissipation leads to the challenge of keeping devices away from overheating. Flow-boiling microchannel heat-sinks exploit the highly efficient thermal energy transport of phase change from liquid to vapor. However, the excessive consumption of liquid-phase by highly localized heat source causes the two-phase flow maldistribution, leading to greatly reduced heat transfer coefficient, high-pressure loss, and limited flow rate. In this study, we investigate two-dimensional flow-boiling morphological characteristics in a microgap with hydrophilic coating on hot-spot. The experiments are carried out on a Stainless Steel plate having a micro gap depth of 254 µm using deionized water with inlet at room temperature. A partial hydrophilic surface is created on the hot-spot (surface above the heater) which forms a wettability difference along the metal plate. A wide range of mass flux and heat flux are considered to quantify heat transfer coefficient. In addition, high-speed flow visualizations are performed to characterize the nucleation and bubble dynamics in flow boiling.

Keywords: Two-phase flow, heat transfer, hydrophilic, flow boiling.

NOMENCLATURE

q	effective heat flux [W/m^2]
h	heat transfer coefficient [W/m^{2}K]
j	mass flux [Kg/m^{2}s]
ΔT	temperature difference [^{0}C]

1. INTRODUCTION

Recently, two-phase flow boiling has become very familiar for high-performance computing devices, defense and aircraft applications as it can remove a large amount of heat from a small area by using latent heat of vaporization [1]. Despite the benefits of dissipating higher heat flux, two-phase flow in narrow spaces encounters some critical problems like premature dry out, flow instability, lower heat transfer coefficient, and pressure drop [2-4]. The accumulation of bubbles at the downstream decreases the mass flux, resulting in pressure drop and increase in wall temperature [4]. Kandlikar [5] showed that boiling incipience affects flow reversal, leading to oscillation in pressure and temperature. The flow reversal phenomenon was also observed due to upstream and downstream vapor [6, 7]. Only a few studies have been carried out to control the flow instability. The insertion of flow restrictor at channel inlet was proposed to stabilize the flow, but the surface temperature increased [8, 9]. Lu et al. [10] and Tamanna et al. [11] made diverging or expanding channel cross-section to control instability. While they showed improvement in flow stability by reducing pressure oscillation, still there was some flow reversal at the inlet. The problem becomes even worse when considering local hot spot in micro channel flow. Local hot spot forms in electronic devices, resulting in a significant increase of peak temperature at the same power level. Researchers have been adopting different techniques in two-phase cooling to address this issue. Choi et al. [12] considered cross-linking of microchannels, providing better temperature uniformity and more effective cooling due to the lateral fluid transport and mixing. In different studies, micro gap cooling was used to mitigate hot spot temperature efficiently [13, 14]. In microgap, vapor gets more space to expand in the transverse and downstream direction and also maintains uniform pressure and fluid film on the hot surface. Alam et al. [15] showed the size effect and flow type in micro gap cooling. They concluded that the heat transfer coefficient increases with smaller micro gap size and heat transfer mechanism are governed by confined slug and annular flow.

Recently, surface wettability attracts attention in micro channel cooling. There are a few studies on the effect of surface wettability in microchannel flow boiling. Liu et al. [16] studied the characteristics of flow boiling on hydrophobic to superhydrophilic microchannels. They observed that on the hydrophilic surface (θ~36^0) new bubbles liked to nucleate, grow, and coalesce into an elongated bubble and then flushed away with incoming water periodically. For hydrophobic surface (θ=103^0) only elongated bubble formed at higher superheat compared to a hydrophilic surface. The heat transfer coefficient is higher for hydrophilic microchannel compared to hydrophobic at low vapor quality and low heat flux but opposite for high vapor quality and heat flux [17, 18]. Choi et al. [18] also mentioned that local dry patches resulted on the hydrophobic surface at low vapor quality and at high vapor quality new nucleation introduced in the unstable liquid film around the elongated bubble on a hydrophobic surface. Some researcher tested a wettability pattern (a mixture of the hydrophilic and hydrophobic surface) effect in flow boiling and found improved heat transfer coefficient and critical heat flux [19, 20].

It has shown improvement in two-phase cooling performance with wetting surface and micro gap heat sinks, but these few studies are not enough to make a strong conclusion about bubble dynamics and dry out phenomena on the hot spot. Moreover, the effect of wetting surface on two-phase micro gap flow in two dimensions has not been studied yet. In the present study, we characterize the change in bubble morphology during flow boiling on hydrophilic hot surface for heat flux range of 24.6 KW/m^2 to 40.9 KW/m^2 at varying mass flux of 0.99 Kg/m^2s to 4.97 Kg/m^2s.

2. EXPERIMENTAL SETUP AND PROCEDURE

2.1 Flow loop

The schematic in Figure 1 represents the experimental setup of this study. The water flow loop is an open loop system. Deionized (DI) water is supplied along the Stainless Steel (SS) heat sink using a syringe pump which has an inbuilt digital flow rate control panel. A fixed volume of 60 mL of DI water is pumped from the syringe. The water first enters into the test piece through the inlet where the temperature of the water is measured. Then it flows along the hot SS plate to remove heat. The water coming out through the outlet is collected in an open container. The temperature and pressure of water are measured using T type thermocouple and absolute pressure sensor before and after it passes the SS heat sink. A differential pressure sensor is set to measure the pressure difference between inlet and outlet.

2.2 Test module

The test module is illustrated in Figure 2. The main test section is comprised of Teflon base plate, Polycarbonate top cover, 28×28 mm stainless steel plate, leaded resistor (heater), and metal brace. The SS metal plate has a shallow depth of 254 µm channel with 19.8 mm width. Due to lower thermal conductivity, SS plate dissipates low heat in surrounding areas, which facilitates to mimic hot spot at the middle. A 100 W AIN leaded resistor (Barry Industries Inc.) is used as a heater which is 8.89×5.84×1.78 mm in dimension. It is mounted on the desired groove of Teflon base. A thermal compound (Chemplex ® 1381 DE) is applied on the heater surface to maintain constant conduction between heater and heat sink. Two 7.62 mm holes are drilled through the Teflon base plate just before inlet and after outlet to attach two absolute (PX219-200A5V) and one differential pressure transducer (PX419-015DWUV). Power is supplied to heater from an AC source with variable voltage level. Total ten T type thermocouples are used to measure the temperature of the heat sink (SS plate) surface in different positions, eight are measuring the local temperature of metal plate from back, one in between the heater and metal plate and the other one is fixed through top polycarbonate part to measure the flowing water temperature above metal plate. The Agilent 34970A data acquisition system records all temperature and pressure data.

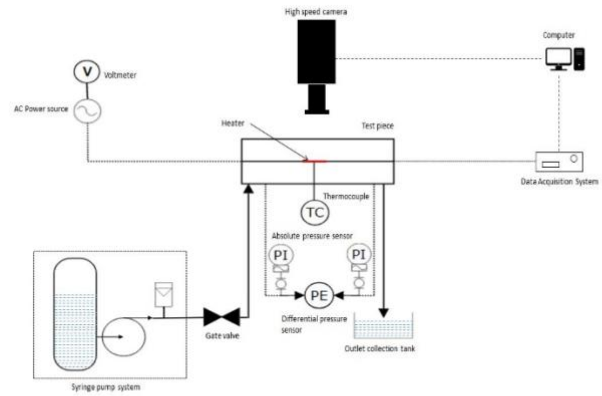

FIGURE 1: SCHEMATIC DIAGRAM OF TEST LOOP.

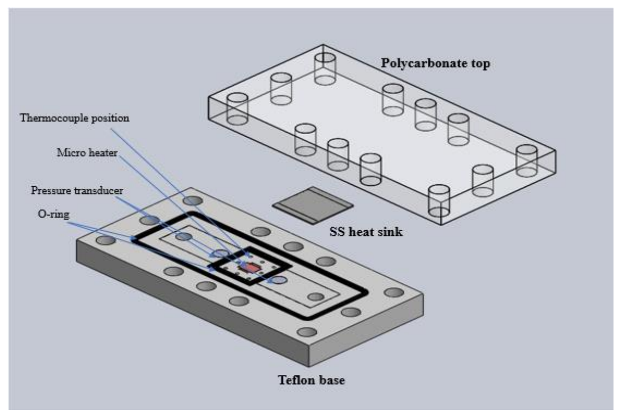

FIGURE 2: ARRANGEMENT AND COMPONENTS OF TEST PIECE.

2.3 Hydrophilic surface treatment

The hydrophilic surface treatment is done using plasma treatment. Small scale plasma treatment setup is shown in Figure 3. The cylinder is maintained air free by injecting Helium gas. The electrode, inside the chamber, is connected to the positive and negative terminal of the high voltage source (10 kV, 30 mA). This power source is connected to the variac transformer (output: 0-30 VAC 60 Hz). 5-7 minutes of plasma treatment on SS surface changes the contact angle of the spot from ~ 87^0 to ~13^0. During plasma treatment, surface undergoes oxidation and plasma bombardment and forms hydroxyl group on the surface. The polar hydroxyl group attracts water and thus fastens the bubble nucleation. The plasma-treated hydrophilic surface has the limitation of deteriorating over time due to heating and water flow. So the contact angle of hydrophilic surface changes over time, which is shown in Figure 4. In this experiment, generally, water starts to boil after an hour and the contact angle during boiling remains in between 44^0 and 48^0. This small change has negligible effect on boiling phenomena.

2.4 Experimental procedure

The metal plate (non-treated and plasma treated) is set to the test section in separate runs, and the test section is connected to the flow loop. The power supply connected to the heater is turned on and maintained at the same power level throughout the experiment. The experiment is continued for different heat fluxes varying from 24.6 to 40 KW/m^2. Once all the thermocouple and pressure readings reached steady state condition for specific heat flux, the syringe pump is started to flow water. Six different flow rates varying from 0.3 mL/min to 1.5 mL/min are used to see the cooling effect for each heat flux. A high-speed camera (Miro M310) is used to visualize the morphological change inside bubbles during flow boiling.

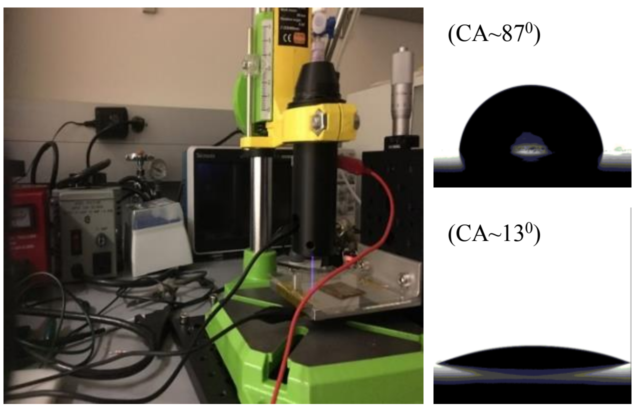

FIGURE 3: PLASMA HYDROPHILIC SURFACE TREATMENT SETUP AND CONTACT ANGLE (CA) MEASUREMENT BEFORE TREATMENT (CA~87^0) [ABOVE] AND AFTER TREATMENT (CA~13^0) [BELOW].

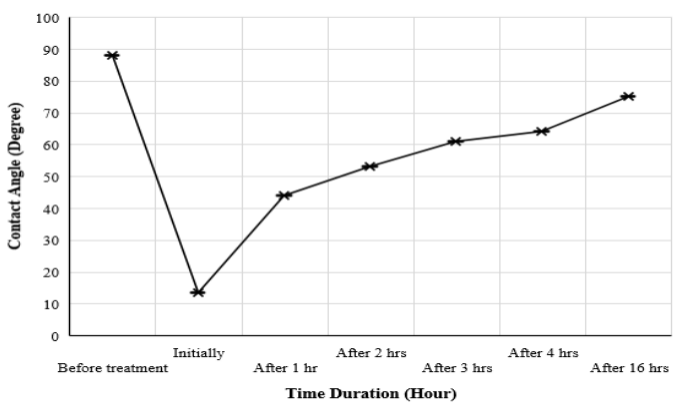

FIGURE 4: VARIATION OF CONTACT ANGLE WITH TIME ON HYDROPHILIC SURFACE

2.5 Heat transfer data analysis

In this experiment, the input power (P) is calculated using voltage (V), *power factor (pf =0.8)* of the power source and the resistance (R) of microheater.

$$P = \frac{V^2 pf}{R} \tag{1}$$

Heat transfer rate (Q) is calculated considering the heat loss (Q_{loss}) to surrounding ambient. The average heat loss with the microheater is around 9% of input power P.

$$Q = P - Q_{loss} \tag{2}$$

Two-dimensional temperature difference (ΔT) is calculated using average wall temperature (T_{wall}) and average water temperature right above the hot surface (T_{water}) for a specific time of $t=1000$ s when the temperature reaches steady state during cooling.

$$\Delta T = T_{wall} - T_{water} \tag{3}$$

Micro heater's surface area (A_h) is considered to calculate effective heat flux (q).

$$q = \frac{Q}{A_h} \tag{4}$$

Two-phase heat transfer coefficient (h) can be calculated using:

$$h = \frac{q}{\Delta T} \tag{5}$$

3. RESULTS AND DISCUSSION

In the present experiment, flow visualization during flow boiling on conventional and hydrophilic surfaces has been performed and also the effect of hydrophilic treatment on the hot spot has been evaluated. The average contact angle was measured around 87^0 for conventional SS plate and approximately 45^0 for plasma treated hydrophilic surface.

3.1 Flow visualization

The flow visualization is performed at boiling incipience using a high-speed camera. Figure 5 illustrates the comparison of the nucleation and bubble growth on conventional and hydrophilic surface.

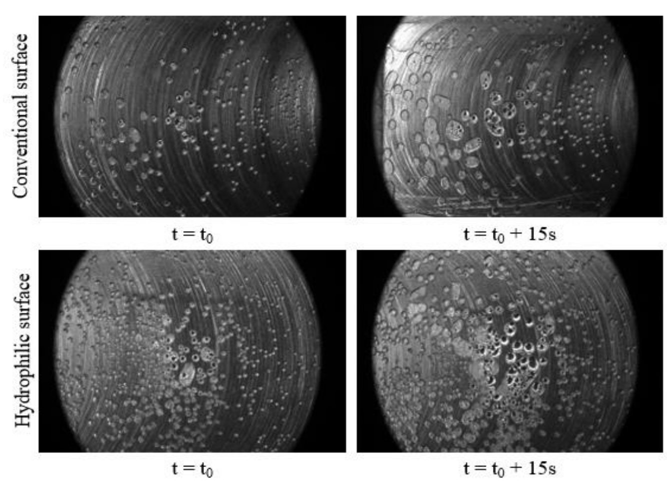

FIGURE 5: COMPARISON OF NUCLEATION AND BUBBLE GROWTH ON CONVENTIONAL AND HYDROPHILIC SURFACE WITH TIME.

The figure clearly shows that a large number of bubbles are formed on hydrophilic surface at $t = t_0$. The bubbles are started to coalesce and elongate after while which is visible at $t = t_0 + 15$ s. This bubble growth rate is also higher on hydrophilic surface. It is due to the higher surface energy of hydrophilic surface which enhances adhesion capability and hence nucleation. At the boiling incipience, the flow type is generally bubbly (like Figure 5) and turns to slug flow when bubble becomes longer. Figure 6 shows the visualization of bubble elongation with time on conventional surface. The bubbles mostly stay at the same position and the elongation rate is also slow. At $t = t_0 + 6.5$ s, bubble started to elongate but no significant elongation is observed before $t = t_0 + 9$ s. At this time bubble started to elongate in the vertical direction. Finally, at $t = t_0 + 14$ s both vertical and horizontal elongation is visible. On conventional surface, bubble cluster elongates and forms slug slowly but it stays mostly at the same location. It is rarely found to move at higher mass flux (4.97 Kg/m^{2}s) only.

On the other hand, a large number of bubbles form slug rapidly and it starts to move very quickly ($t = t_0 + 6$ s) in case of hydrophilic surface shown in Figure 7. The elongation and movement of slug is clearly visible at $t = t_0 + 7.5$ s and $t = t_0 + 15$ s. Due to the hydrophilicity, incoming water flushes this bubble slug and fills the hot spot. Figure 8 identifies this clearly. The new incoming water removes the vapor slug from the hot spot very quickly (in only 2.56 s). This phenomenon is consistent with the study of Liu et al. [16]. It is also found that in this vapor slug larger bubbles collapse and form smaller bubbles more frequently.

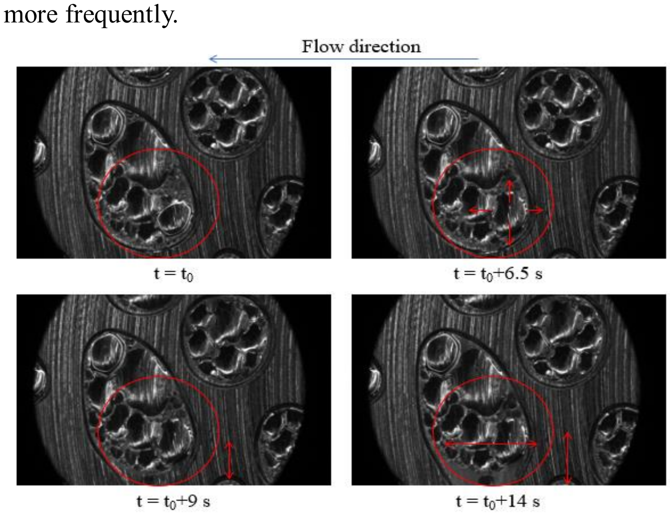

FIGURE 6: BUBBLE ELONGATION AND MOVEMENT ON CONVENTIONAL SURFACE WITH TIME.

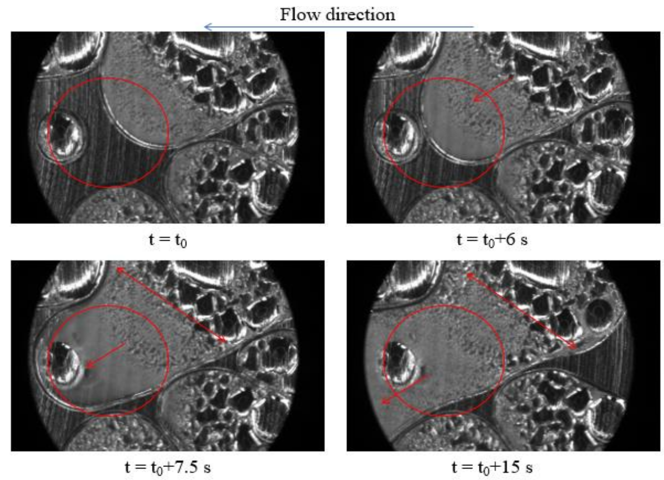

FIGURE 7: BUBBLE ELONGATION AND MOVEMENT ON HYDROPHILIC SURFACE WITH TIME.

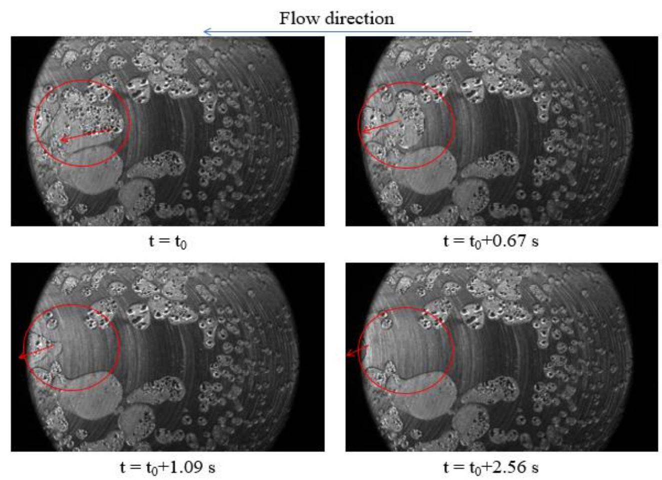

FIGURE 8: FLUSHING OF VAPOR SLUG ON HYDROPHILIC SURFACE WITH TIME.

3.2 Cooling performance

The temperature distribution along the heat sink at the end of cooling for conventional and hydrophilic surface is shown in Figure 9. It is evident from the figure that the temperature of the hot wall (above heater) is significantly dropped (88.45^{0}C) on hydrophilic surface compared to conventional surface (109.33^{0}C). The wall and water temperature variation right above hot spot for $q=2.84\times10^4$ W/m^2 and $j=3.98$ Kg/m^{2}s are illustrated in Figure 10. The temperature distribution for the hydrophilic surface looks oscillatory compared to conventional surface. Due to flushing of vapor slug, new water prevails on the hot spot and remains single phase before introducing new bubble nucleation. It makes the wall and water temperature profile cyclic and oscillatory for the hydrophilic surface. This phenomenon is also found by Liu et al. [16] and Wang et al. [19]. The higher water temperature and lower wall temperature of hydrophilic surface compared to conventional surface denote the higher heat transfer on hydrophilic surface. It also implies that water takes out more heat from the hot spot of the hydrophilic surface and improves cooling performance.

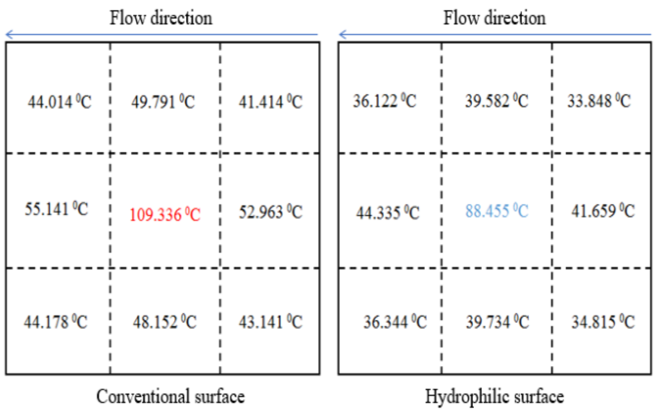

FIGURE 9: COMPARISON OF TEMPERATURE DISTRIBUTION ON HEAT SINK AT THE END OF COOLING FOR CONVENTIONAL AND HYDROPHILIC SURFACE AT $q=2.84\times10^4$ W/m^2 AND $j=3.98$ KG/m^2s.

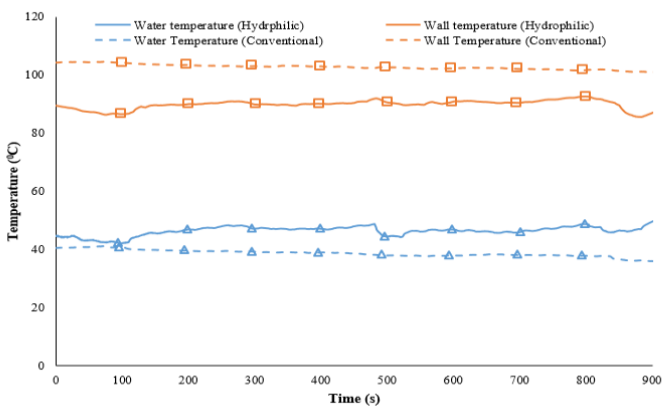

FIGURE 10: WALL AND WATER TEMPERATURE VARIATION ON HOT SPOT FOR CONVENTIONAL AND HYDROPHILIC SURFACE AT $q=2.84\times10^4$ W/m^2 AND $j=3.98$ KG/m^2s.

3.3 Two phase Heat transfer coefficient

Figure 11 shows the variation of effective heat flux with temperature difference for different mass fluxes. It is interesting to see that at low heat flux ($<3\times10^4$ W/m^2) temperature difference is significantly lower for the hydrophilic surface than conventional, but it becomes opposite for higher heat flux ($\sim4.1\times10^4$ W/m^2). This is also consistent with Figure 12. It illustrates that the heat transfer coefficient decreases with the heat flux in case of hydrophilic surface, but the opposite happens for the conventional surface. The studies of Trieu et al. [17] and Choi et al. [18] also reported the decrease of heat transfer coefficient on the hydrophilic surface at high heat flux. Trieu et al. [17] mentioned in their study that at high vapor quality or heat flux the dominance of capillary effects on the hydrophilic surface keeps the liquid film thickness partially unchanged that enhances temperature difference and decreases heat transfer.

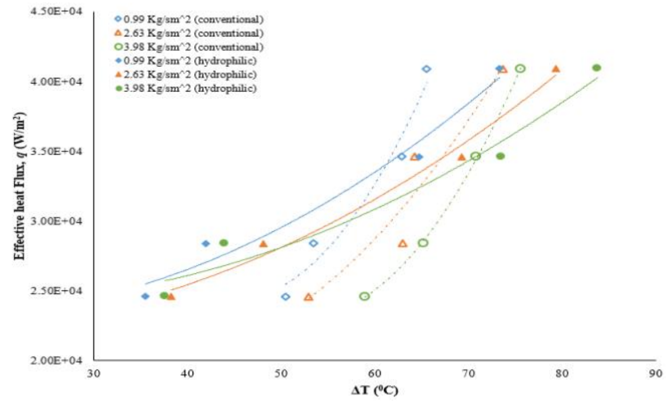

FIGURE 11: VARIATION OF EFFECTIVE HEAT FLUX WITH TEMPERATURE DIFFERENCE ON CONVENTIONAL AND HYDROPHILIC SURFACE FOR VARIOUS MASS FLUXES.

It is also noticed that the heat transfer coefficient decreases with the increase of mass flux for both conventional and hydrophilic surface. Fig 12 also shows that the heat transfer coefficient data varies more around the trend for hydrophilic surface compared to conventional one. This could happen due to the short durability of hydrophilicity. As plasma hydrophilic treatment deteriorates with time depending on mass flux, it shows little bias around the trend.

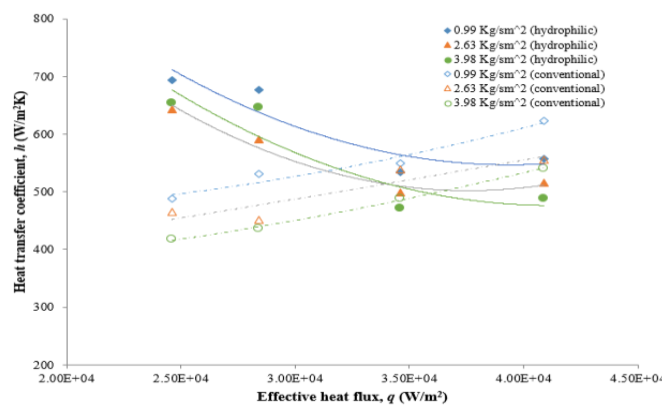

FIGURE 12: VARIATION OF HEAT TRANSFER COEFFICIENT WITH EFFECTIVE HEAT FLUX ON CONVENTIONAL AND HYDROPHILIC SURFACE FOR VARIOUS MASS FLUX.

4. CONCLUSION

This experimental investigation is carried out to characterize the comparative morphological change and the change in temperature and pressure on the non-treated, and hydrophilic treated hot spot of SS microgap heat sink in two-phase cooling. To evaluate the heat transfer coefficient on these surfaces different mass flux varying from 0.99 Kg/m^2s to 4.97 Kg/m^2s at different heat flux varying from 24.6 KW/m^2 to 40.9 KW/m^2 are considered. The flow visualization shows the flow transition from bubbly to slug flow in this flow boiling. The vapor slug flushes away by incoming water from the hot spot for hydrophilic treated surface while it remains static on the conventional surface. Hydrophilic treated surface provides improved cooling performance with oscillatory temperature profile. The average differential pressure on hydrophilic treated surface is lower than the conventional surface as it maintains the almost uniform pressure difference between inlet and outlet by reducing flow instability. Heat transfer coefficient decreases with the increment of heat flux for hydrophilic surface and opposite happens for the conventional surface. For low mass flux, heat transfer coefficient is higher in both the cases.

ACKNOWLEDGMENTS

This work was supported by the National Science Foundation under Grant No. 1707056.

REFERENCE

[1] Jaeseon Lee, and Mudawar, I., 2009, "Low-Temperature Two-Phase Microchannel Cooling for High-Heat-Flux Thermal Management of Defense Electronics", IEEE Transactions on Components and Packaging Technologies, 32(2), pp. 453-465.

[2] Bergles, A.E. Mayinger, F. (Ed.). (1977). Review of instabilities in two-phase systems. United States: Hemisphere Publishing Corp.

[3] Tadrist, L., 2007, "Review on two-phase flow instabilities in narrow spaces", International Journal of Heat and Fluid Flow, 28(1), pp. 54-62.

[4] Qi, S., Zhang, P., Wang, R., and Xu, L., 2007, "Flow boiling of liquid nitrogen in micro-tubes: Part I – The onset of nucleate boiling, two-phase flow instability and two-phase flow pressure drop", International Journal of Heat and Mass Transfer, 50(25-26), pp. 4999-5016.

[5] Kandlikar, S., 2006, "Nucleation characteristics and stability considerations during flow boiling in microchannels", Experimental Thermal and Fluid Science, 30(5), pp. 441-447.

[6] Hetsroni G., Klein D., A. Mosyak, Z. Segal & E. Pogrebnyak, 2004 "Convective boiling in parallel microchannels, Microscale Thermophysical Engineering, 8:4, 403-421.

[7] Peles YY. Two-Phase Boiling Flow in Microchannels: Instabilities Issues and Flow Regime Mapping. ASME. International Conference on Nanochannels, Microchannels, and Minichannels, 1st International Conference on Microchannels and Minichannels ():559-566.

[8] Koşar A, Kuo C, Peles Y. Suppression of Boiling Flow Oscillations in Parallel Microchannels by Inlet Restrictors. ASME. J. Heat Transfer. 2005;128(3):251-260.

[9] Kuan, W., and Kandlikar, S., 2007, "Experimental Study on the Effect of Stabilization on Flow Boiling Heat Transfer in Microchannels", Heat Transfer Engineering, 28(8-9), pp. 746-752.

[10] Lu, C., and Pan, C., 2008, "Stabilization of flow boiling in microchannel heat sinks with a diverging cross-section design", Journal of Micromechanics and Microengineering, 18(7), p. 075035.

[11] Tamanna, A., and Lee, P., 2015, "Flow boiling instability characteristics in expanding silicon microgap heat sink", International Journal of Heat and Mass Transfer, 89, pp. 390-405.

[12] Cho E.S., Koa J.M., Jiang L., Prasher R.S., Kim M.S., Santiago J.G., Kenny T.W., Goodson K.E., Experimental study on two-phase heat transfer in microchannel heat sinks with hotspots, in: Semiconductor Thermal Measurement and Management Symposium, 2003, pp. 242–246.

[13] Bar-Cohen, A., and Wang, P., 2012, "Thermal Management of On-Chip Hot Spot", Journal of Heat Transfer, 134(5), p. 051017.

[14] Alam, T., Lee, P., Yap, C., and Jin, L., 2013, "A comparative study of flow boiling heat transfer and pressure drop characteristics in microgap and microchannel heat sink and an evaluation of microgap heat sink for hotspot mitigation", International Journal of Heat and Mass Transfer, 58(1-2), pp. 335-347.

[15] Alam, T., Lee, P., Yap, C., and Jin, L., 2012, "Experimental investigation of local flow boiling heat transfer and pressure drop characteristics in microgap channel", International Journal of Multiphase Flow, 42, pp. 164-174.

[16] Liu, T., Li, P., Liu, C., and Gau, C., 2011, "Boiling flow characteristics in microchannels with very hydrophobic surface to super-hydrophilic surface", International Journal of Heat and Mass Transfer, 54(1-3), pp. 126-134.

[17] Trieu Phan, H., Caney, N., Marty, P., Colasson, S., and Gavillet, J., 2012, "Flow Boiling of Water on Nanocoated Surfaces in a Microchannel", Journal of Heat Transfer, 134(2), p. 020901.

[18] Choi, C., Shin, J., Yu, D., and Kim, M., 2011, "Flow boiling behaviors in hydrophilic and hydrophobic microchannels", Experimental Thermal and Fluid Science, 35(5), pp. 816-824.

[19] Wang B., He M., Wang H. and Qiu H., "Flow boiling heat transfer in wettability patterned microchannels," 2017 16th IEEE Intersociety Conference on Thermal and Thermomechanical Phenomena in Electronic Systems (ITherm), Orlando, FL, 2017, pp. 759-766.

[20] Kim, J., Kang, S., Yu, D., Park, H., Moriyama, K., and Kim, M., 2017, "Smart surface in flow boiling: Spontaneous change of wettability", International Journal of Heat and Mass Transfer, 105, pp. 147-156.

